GEOPHYSICAL RESEARCH LETTERS, VOL. 26, NO.6, PAGES 663-666, MARCH 15, 1999

Discrete Auroral Arcs and Nonlinear Dispersive Field Line Resonances

R. Rankin, J. C. Samson, and V. T. Tikhonchuk[1]

Department of Physics, University of Alberta, Edmonton, Canada

Abstract. Dispersive effects in field line resonances (FLRs) are discussed in the context of potential structures, parallel currents, and auroral density cavities observed by the FAST satellite. Our model includes the Earth's dipole magnetic field, and accounts for electron inertia, electron thermal pressure, finite ion gyroradius effects, and field aligned variations of the plasma density and ambient electron and ion temperatures. For realistic backgound parameters, we show that finite plasma temperature effects determine the dynamics of FLRs and that solitary wave structures evolve out of the resonance region, producing deep density cavities above the polar ionospheres. Results are shown to be in reasonable agreement with ground and satellite observations, with the exception of the magnitude of low altitude electric fields.

Introduction

Field line resonances (FLRs) are standing shear Alfvén waves (SAWs) in the Earth's magnetosphere, and are a common feature seen in magnetometer, radar, and optical data in the ULF frequency range $1-4$ mHz [*Samson et al.*, 1991]. Here, we shall discuss results based on a model [*Rankin et al.*, 1998] of nonlinear, dispersive SAWs that describes electromagnetic field perturbations, plasma density cavities, electric currents and particle precipitation in the auroral region. The results from this model suggest that FLRs might provide a unified explanation for recent satellite observations of certain features of auroral activity [*Lundin et al.*, 1994; *Persoon et al.*, 1988; *Stasiewicz et al.*, 1997; *Lotko et al.*, 1998].

Dispersion in SAWs arises through electron inertia at altitudes below $1R_e$, and through electron thermal pressure and ion gyroradius effects at higher altitudes, in the vicinity of the equatorial magnetosphere. *Hasegawa* [1976] and *Goertz* [1984] have shown that electron inertia in SAWs can generate a parallel electric field which can accelerate particles above the auroral ionosphere. *Streltsov and Lotko* [1997] have shown that in a dipolar magnetic field, plasma parallel inhomogeneity can enhance SAW electric and magnetic fields. More recently, *Lotko et al.* [1998] have discussed a 4100 km altitude FAST satellite pass through a structure that was interpreted as a 1.3 mHz FLR. To obtain agreement with the observations, *Lotko et al.* [1998] imposed a low altitude density cavity in their linear dispersive FLR model, used an FLR frequency that was 8-9 times larger than the observed 1.3 mHz, neglected ionospheric conductivity, and added an ad-hoc anomalous resistive layer that leads to a large highly localized electric field that is consistent with FAST measurements. Without these assumptions, and in the absence of ionospheric damping, the perpendicular width of the SAW contracts to very short scales, and parallel electric fields are generated which are much too small.

While *Lotko et al.*, [1998] have identified some of the underlying physics in the FAST results, it is also important to determine the saturated nonlinear state of a dispersive FLR using self-consistent nonlinear models. It has previously been demonstrated that the ponderomotive force (PF) is the dominant nonlinear effect on SAWs in the auroral zone. As shown in *Frycz et al.* [1998] and *Rankin et al.* [1998], the PF can nonlinearly saturate dispersive FLRs through the excitation of large amplitude standing ion acoustic waves. These waves are associated with density cavities near the ionosphere, and can produce nonlinear dispersive-scale FLR structuring in the radial direction.

In *Frycz et al.* [1998] and *Rankin et al.* [1998] two nonlinear regimes were identified which depend on whether dispersion is dominated by electron inertia or finite temperature effects. In the electron inertia regime, dispersion and nonlinearity result in a parametric decay instability (PDI) of SAWs into secondary SAWs and ion acoustic waves. This instability evolves exponentially in time, with its own nonlinear space and timescales. For inner magnetosphere parameters, thermal effects dominate dispersion, and the PDI is forbidden. However, the excited SAW is observed to emit solitons periodically from the resonance region. This process does not involve instability, and therefore has no threshold or matching constraints. We note also that in the auroral ionosphere, density modulations created by Alfvén waves can strongly influence lower-hybrid waves [*Wahlund et al.*, 1994] through modulational coupling and collapse. This instability may require consideration when comparing density perturbations generated through the PDI. Here, we shall present results of modeling for typical parameters of magnetospheric FLRs, and discuss the observational capabilities of the model. Our model can explain many features of the observations, including the approximate magnitudes of field aligned currents and density perturbations, the existence of a low altitude density cavity, and the transverse scale of wave fields.

The Model for a Nonlinear Dispersive Dipolar FLR

Our nonlinear, dispersive, dipolar (NDD) model of FLR dynamics describes the nonlinear interaction between a standing SAW (resonantly driven by an external source) and a spectrum of standing ion acoustic waves in a dipole geometry. The governing equations can be found in [*Rankin et*

[1]On leave from the P. N. Lebedev Physics Institute, Russian Academy of Sciences, Moscow.

Paper number 1999GL900058.
0094-8276/99/1999GL900058$05.00

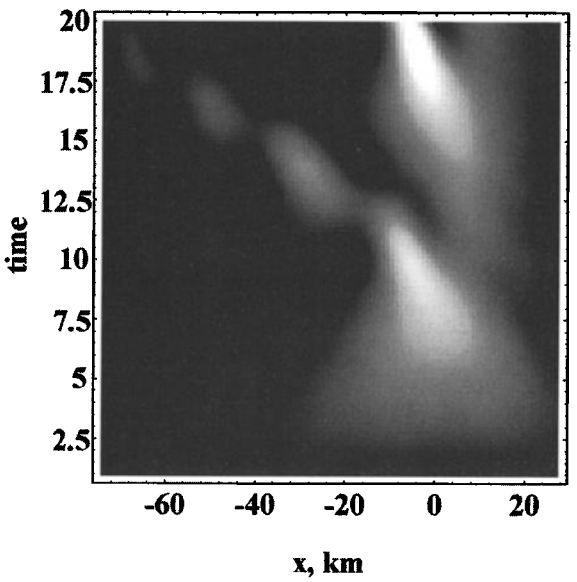

Figure 1. Gray scale plot showing the radial and time dependence of the azimuthal magnetic field amplitude near the ionosphere. Parameters of the model are described in the text. Time is measured in SAW periods, positive x corresponds to the equatorward direction.

al., 1998]. The azimuthal magnetic field is represented as $B_\phi = (B_0^{eq}/h_\phi)\mathrm{Re}\, b(x,t)\, S_1(l)\, \exp i(m\phi - \omega_0 t)$, where l is the field-aligned coordinate, $h_\phi(l)$ is the metric factor that accounts for the compression of the azimuthal magnetic flux near the ionospheres, B_0^{eq} is the ambient (dipolar) equatorial magnetic field, and m is the azimuthal SAW mode number. We consider a low-m case and neglect the excitation of poloidal SAW components. The driver frequency, ω_0, is resonant with the fundamental SAW mode of frequency $\omega_1(x)$ at $x = 0$, where x is the radial coordinate in the equatorial plane. The SAW toroidal eigenmode, $S_1(l)$, and eigenfrequency were calculated by *Taylor and Walker* [1984], and *Cheng et al.* [1993]. The SAW amplitude, b, satisfies the nonlinear Schrödinger equation *[Frycz et al.*, 1998; *Rankin et al.*, 1998]:

$$\frac{\partial b}{\partial t} - i\frac{\omega_0}{2}\delta\frac{\partial^2 b}{\partial x^2} = i\,(\delta\Omega - \Delta\omega)\, b + \frac{\omega_0}{2}R. \qquad (1)$$

Here, $\Delta\omega(x) = \omega_1(x) - \omega_0 = \omega_0 x/2l_\omega - i\gamma_{SAW}$ is a linear function of the radial coordinate, with an imaginary part, γ_{SAW}, that accounts for ionospheric damping [*Taylor and Walker*, 1984; *Samson et al.*, 1996]. The source term, R, represents the amplitude of the compressional Alfvén wave driver at the resonance layer, and δ characterizes the dispersive properties of the SAW averaged along the magnetic field line,

$$\delta = \int \frac{dl}{h_\mu}\left[\frac{3\rho_i^2 V_A^2}{4\omega_0^2}\left(\frac{\partial S_1}{\partial l}\right)^2 + \frac{V_{Te}^2}{\omega_0^2}\frac{\partial S_1}{\partial l}\frac{\partial S_1 \lambda_e^2}{\partial l} - \lambda_e^2 S_1^2\right]. \qquad (2)$$

Here, all parameters in the integrand are functions of position along the field line: ρ_i is the ion gyroradius, λ_e is the electron inertia length, V_{Te} is the electron thermal velocity, V_A is the Alfvén velocity, and $h_\mu(l)$ is the field aligned metric coefficient. The SAW eigenfunction is normalized according to $\int dl\, S_1^2 h_\mu/h_\phi^2 = L^4 R_e^4$ where L denotes the resonant magnetic shell and R_e is the Earth's radius. The sign

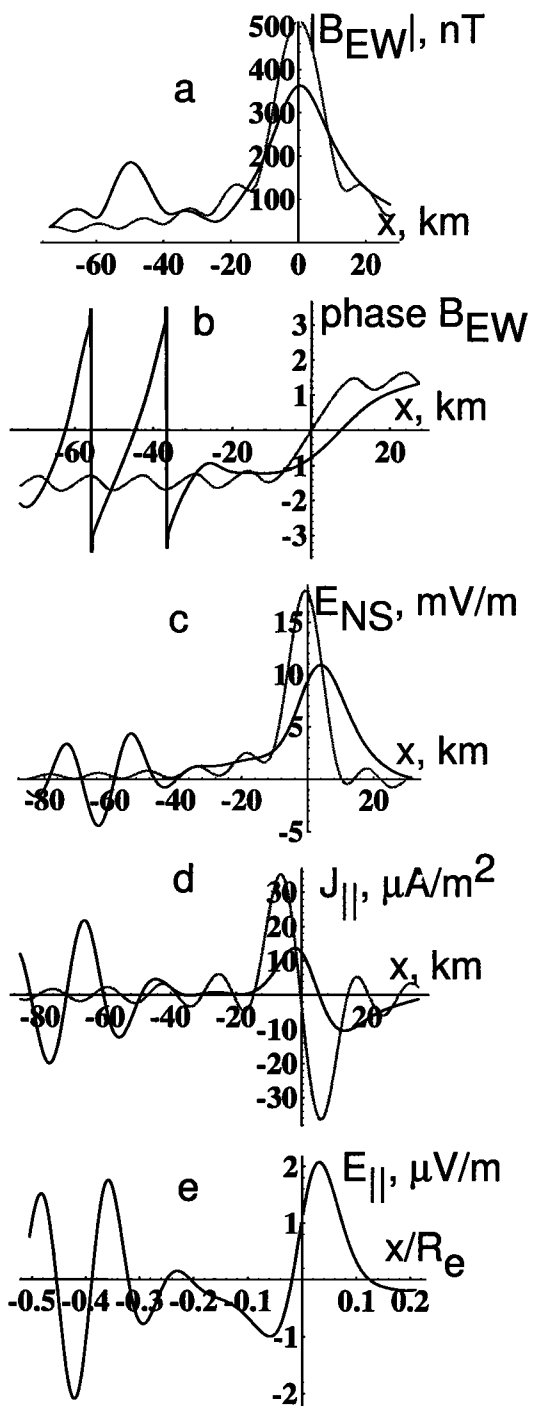

Figure 2. Radial cross-sections of the azimuthal magnetic field amplitude (a) and phase (b) near the ionosphere at a time of 17 SAW periods. Gray lines show the results of the linear, nondispersive model. Panels c and d represent radial cuts of the radial electric field and parallel electron current near the ionosphere; panel e shows the parallel electric field at the distance $2.5R_e$ from the equatorial plane where it achieves its maximum value.

of δ depends on the ambient plasma parameters. Negative δ corresponds to the dominance of electron inertia, while positive δ indicates the dominance of electron thermal pressure and ion gyroradius effects.

The nonlinear SAW frequency shift, $\delta\Omega = (1/2)\omega_0 \sum_M n_M g_M$, is due to ponderomotively driven density per-

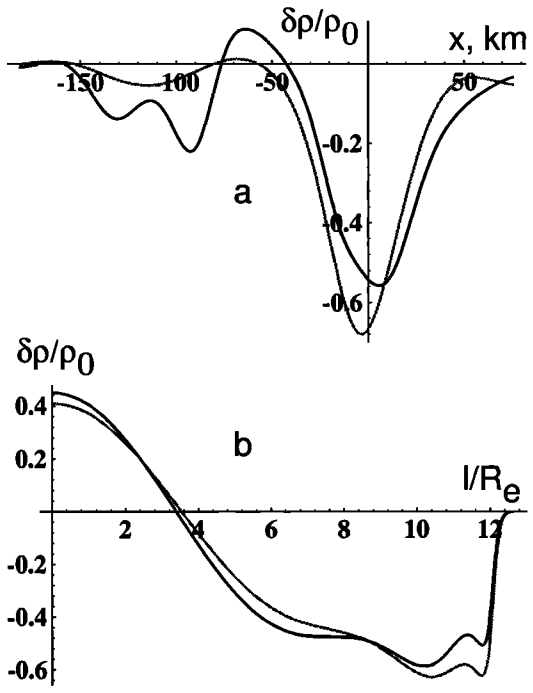

Figure 3. Radial (a) and parallel (b) cuts of the relative density perturbation for time moments of 10 (gray lines) and 17 (solid lines) SAW periods. Radial cuts correspond to an altitude 1 R_e above the Earth; parallel cuts are made at the original FLR position, $x = 0$.

turbations. The latter are represented as a linear combination of ion acoustic wave eigenmodes, $\delta\rho = \rho_0^{eq}(l) \sum_M n_M(x,t) U_M(l)$ where $U_M(l)$ are the ion acoustic wave eigenfunctions [*Cheng et al.*, 1993; *Rankin et al*, 1998]. The harmonic amplitudes satisfy an ion acoustic wave equation that is driven by the PF:

$$\frac{\partial^2 n_M}{\partial t^2} + 2\Gamma_{IAW}\Omega_M \frac{\partial n_M}{\partial t} + \Omega_M^2 n_M = \frac{\omega_0^2}{2} f_M |b|^2, \qquad (3)$$

where Ω_M is the ion acoustic wave eigenfrequency, Γ_{IAW} is the damping coefficient, and coefficients g_M and f_M describe the coupling efficiency between the SAW and ion acoustic waves.

Background Parameters

Eqs. (1) and (3) describe the nonlinear evolution and saturation of coupled, dispersive SAWs and ion acoustic waves. In solving them, our choice of plasma profiles is guided by *Streltsov and Lotko* [1997]. We consider the density profile $\rho_0(\theta) = \rho_0^{eq} p(\theta)$, and the temperature profile $T(\theta) = T^{eq}/p(\theta)$ with $p(\theta) = 0.77 + 0.23\cos^{-6}\theta + 1.7 \cdot 10^5 \exp[-(L\cos^2\theta - 1.05)/0.08]$ where θ is the magnetic latitude and $L\cos^2\theta$ is the geocentric distance in Earth radii. The last, exponential term accounts for the density increase in the polar magnetosphere due to oxygen emission from the ionosphere. We assume a constant ratio of 3 : 2 between hydrogen and oxygen, and an $L = 10$ FLR with an equatorial plasma density $\rho_0^{eq} = 7$ amu/cm^3. Electrons and ions have the same temperature profile with $T_i^{eq} = 200$ eV and $T_e^{eq} = 100$ eV. The height integrated Pedersen conductivity is assumed to be 20 mho and the ion damping coefficient, $\Gamma_{IAW} = 0.3$.

The above parameters give a fundamental SAW eigenmode with a period of 12.7 min (frequency 1.3 mHz) and a damping time of 137 min, and are in qualitative agreement with observations [*Samson et al.*, 1996; *Lotko et al.*, 1998]. The dispersion parameter $\delta = 3.6 \cdot 10^{-4} R_e^2$ is positive, which indicates the dominance of ion gyroradius and electron thermal effects in the equatorial plane. The periods of the first three even ion acoustic wave eigenmodes, which dominate the ion acoustic wave response, are 27.2, 15.0, and 10.5 min, respectively. In calculating these periods, we have accounted for perpendicular dispersion $\sim (C_S/V_A)^2$ [*Cheng et al.*, 1993; *Rankin et al.*, 1998], but have neglected their radial dependence because the variation of ion wave periods is small on the FLR characteristic scale.

NDD Model Results

We use a compressional wave amplitude of a few nT in the equatorial plane [$R = 0.016$ in Eq. (1)]. The evolution of the FLR magnetic field amplitude near the ionosphere is shown in Fig. 1. The first stage of linear FLR excitation takes about $5-7$ SAW periods, after which the FLR enters a nonlinear phase. It consists of periodic saturation and emission of narrow localized SAW solitons which propagate slowly poleward (shift ~ 5 km per one SAW period). The pulsating dynamics of the FLR is a result of competition between SAW dispersion (dominated by the ion gyroradius effect) and the ponderomotive nonlinearity. The maximum amplitude of the SAW azimuthal (East- West, EW) magnetic field is ~ 350 nT compared to 500 nT which one obtains from linear saturation due to SAW dissipation [with nonlinearity and dispersion both neglected in Eq. (1)] at the polar ionospheres. The saturated FLR also has a very specific phase structure: the nonshifted peak in Fig. 2b (dark line) is the usual π-shift signature of a linear FLR (gray line in Fig. 2b), while the shifted peak demonstrates a 2π shift, corresponding to finite Poynting flux carried by solitons out of the resonance.

The NDD model predicts that the ratio of the radial (North-South, NS) electric field, E_{NS}, to the azimuthal magnetic field near the ionosphere, $|E_{NS}/B_{EW}| = 1/\mu_0\Sigma_P$, depends only on the height integrated Pedersen conductivity. Here, E_{NS} is due to the quadrature component of the electric field, which dominates at the ionospheric ends [*Samson et al.*,1996] and drives Poynting flux into the ionosphere. According to Fig. 2c, the saturated amplitude of E_{NS} is small, about 10 mV/m, compared to measured satellite values [*Lotko et al.*, 1998]. To increase E_{NS}/B_{EW}, one might try smaller Σ_P, but the increased damping leads to a broader resonance, smaller B_{EW}, and results in even lower E_{NS}. The perpendicular electric potential drop across the FLR is around $3-4$ kV near the equatorial plane, and is consistent with satellite observations.

The typical width of the saturated FLR is about 10 km (cf. Fig. 2) and is approximately the same for the linear and NDD models. The maximum current density $J_\parallel \approx 25\,\mu$A/m^2 in the NDD model and about 35 μA/m^2 in the linear model. However, the radial structure of the parallel current is different. In the NDD model the parallel current is associated with the SAW soliton and moves with it out of the resonance. The magnitude of the current is consistent with many observations. However, the corresponding electron kinetic energy flux is relatively small (maximum

$\sim 15\,\mu W/m^2$ at an altitude $\sim 1R_e$) because of small electron drift velocity. The maximum electron drift velocity of about 1000 km/s (energy around 4 eV) is achieved at $1R_e$ altitude. The small electron energy along the magnetic field is a consequence of the high plasma parallel conductivity, $\sigma_\parallel = J_\parallel/E_\parallel \sim \epsilon_0\omega_{pe}^2/\omega_0$ where ω_{pe} is the electron plasma frequency. It achieves its minimum at altitudes of a few R_e where the electron inertia effect dominates the electron response. However, the electron density is already high at these altitudes and no significant $E_\parallel$ is generated. In this region, the parallel electric field achieves its maximum value of a few μV/m (cf. Fig. 2e) corresponding to an electron energy less than 100 eV, which is not sufficient for the initiation of significant auroral optical emission.

An important feature of the NDD model is the generation of density perturbations due to the SAW ponderomotive force. This is shown in Fig. 3 at the time of FLR saturation. A density cavity is produced along the magnetic field line from a distance that is $4-5R_e$ from the equatorial plane to altitudes $\sim$ 3000 km above the Earth. Although the absolute value of the density depletion increases toward the Earth, the relative density perturbation, $\delta\rho/\rho_0$, dramatically decreases above the auroral ionosphere. Relative density perturbations up to -1 can be easily achieved for the present set of parameters and one could expect that very deep density cavities could be driven in FLRs although a more accurate, full 2D solution is required in this case [*Rankin*, 1994].

Conclusions

We have presented a nonlinear dispersive dipole (NDD) model of FLRs that accounts for linear and nonlinear saturation processes, the formation of density cavities, parallel and perpendicular electric fields, and field aligned currents. The only free parameter is the strength of the compressional driver that excites SAWs. The model is successful in predicting approximate magnitudes of azimuthal magnetic fields, parallel electron currents, and field aligned density cavities. It also provides good estimates of the radial scale of saturated field quantities, and a reasonable time scale of FLR nonlinear evolution. For a magnetospheric L-shell of 10, the model shows that dispersion is dominated by finite electron thermal pressure and ion gyroradius effects, both of which result in lower parallel electric fields in the auroral zone.

Two problems are unresolved in existing linear and the present NDD models of FLRs. First, the models predict low amplitudes of electric fields in the lower altitude magnetosphere, and, second, the energy flux of precipitating electrons and the electron energy are not sufficient to excite optical auroral emission. An additional mechanism is therefore required which will allow the transfer of a part of FLR energy into the kinetic energy of accelerated electrons. The NDD model indicates the possible location of the acceleration mechanism: this is the expected location where the electron parallel velocity achieves its maximum value, although the electron drift velocity in the current NDD model is found to be small.

It is possible that increased electron energization in the acceleration region can occur if ponderomotively excited large amplitude density perturbations satisfy $|\delta\rho|/\rho_0 \sim 1$. In the present NDD model we do not account for large density perturbations in our calculation of the parallel current. However, the NDD model indicates that large parallel currents are collocated with potentially very large density perturbations. The parallel electric conductivity in deep density cavities will become very low, and the electron drift velocity will have to increase to much larger levels to preserve the same electric current. A 90% density depletion will require a ten times larger electron drift velocity for the same current, bringing the electron energy to the keV level, and requiring parallel electric fields in the mV/m range, assuming an electron acceleration length of a few tenths of an R_e. This idea is currently being addressed in a non perturbative nonlinear model of FLRs.

Acknowledgments. Research for this project has been supported by the Canadian Space Agency, the Natural Science and Engineering Research Council of Canada, NSERC, and the Russian Foundation for Basic Research.

References

Cheng, C. Z., T. C. Chang, C. A. Lin, and W. H. Tsai, Magnetohydrodynamic theory of field line resonances in magnetosphere, *J. Geophys. Res., 98,* 11,339, 1993.

Frycz, P., R. Rankin, J. C. Samson, and V. T. Tikhonchuk, Nonlinear Field Line Resonances: Dispersive Effects, *Phys. Plasmas, 5,* in press, 1998.

Goertz, C. K., Kinetic Alfvén waves on auroral field lines, *Planet. Space Sci., 32,* 1387, 1984.

Hasegawa, A., Particle acceleration by MHD surface wave and formation of aurora, *J. Geophys. Res., 81,* 5083, 1976.

Lotko, W., A. V. Streltsov, and C. W. Carlson, Discrete auroral arc, electrostatic shock and suprathermal electrons powered by dispersive, anomalously resistive field line resonance, *Geophys. Res. Lett.*, submitted, 1998.

Lundin, R., L. Eliasson, G. Haerendel, M. Boehm, and B. Holback, Large scale auroral density cavities observed by Freja, *Geophys. Res. Lett., 21,* 1903, 1994.

Persoon, M., D. A. Gurnett, W. K. Peterson, J. H. Waite, Jr, J. L. Burch, and J. L. Green, Electron density depletions in the nightside auroral zone, *J. Geophys. Res., 93,* 1871, 1988.

Rankin, R., P. Frycz, V. T. Tikhonchuk, and J. C. Samson, Nonlinear standing shear Alfvén waves in the Earth's magnetosphere, *J. Geophys. Res., 99,* 21,291, 1994.

Rankin, R., J. C. Samson, V. T. Tikhonchuk, and I. Voronkov, Auroral density fluctuations on dispersive field line resonances, *J. Geophys. Res., in press,* 1998.

Samson, J. C., T. J. Hughes, F. Creutzberg, D. D. Wallis, R. A. Greenwald, and J. M. Ruohoniemi, Observations of detached, discrete arc in association with field line resonances, *J. Geophys. Res., 96,* 15,683, 1991.

Samson, J. C., L. L. Cogger, and Q. Pao, Observations of field line resonances, auroral arcs, and auroral vortex structures, *J. Geophys. Res., 101,* 17,373, 1996.

Stasiewicz, G. Gustafsson, G. Marklund, P.-A. Lindqvist, J. Clemmons, and L. Zanetti, Cavity resonators, and Alfvén resonance cones observed on Freja, *J. Geophys. Res., 102,* 2565, 1997.

Streltsov, A., and W. Lotko, Dispersive, nonradiative field line resonances in a dipolar magnetic field geometry, *J. Geophys. Res., 102,* 27,121, 1997.

Taylor, J. P. H. and A. D. M. Walker, Accurate approximate formulae for toroidal standing hydromagnetic oscillations in a dipolar geomagnetic field, *Planet. Space Sci., 32,* 1119, 1984.

Wahlund, J.-E, P. Louarn, T. Chust, H. de Feraudy, A. Roux, B. Holback, P.-O. Dovner, and G. Holmgren, *Geophys. Res. Lett., 21,* 1831, 1994.

R. Rankin, J. C. Samson, and V. T. Tikhonchuk, Department of Physics, University of Alberta, Edmonton, T6G 2J1, Canada. (rankin@space.ualberta.ca)

(Received October 5, 1998; revised January 7, 1999; accepted January 7, 1999.)